



1

2

## On the annual variability of

3

## Antarctic aerosol size

4

## distributions at Halley research

5

## station

6

7 Thomas Lachlan-Cope<sup>1</sup>, David Beddows<sup>2</sup>, Neil Brough<sup>1</sup>, Anna E.  
8 Jones<sup>1</sup>, Roy M. Harrison<sup>2,+</sup>, Angelo Lupi<sup>3</sup>, Young Jun Yoon<sup>4</sup>, Aki  
9 Virkkula<sup>5,6</sup> and Manuel Dall'Osto<sup>7\*</sup>

10

11 <sup>1</sup>British Antarctic Survey, NERC, High Cross, Madingley Rd, Cambridge, CB3  
12 0ET, United Kingdom

13 <sup>2</sup>National Center for Atmospheric Sciences, University of Birmingham,  
14 Edgbaston, Birmingham, B15 2TT, United Kingdom

15 <sup>3</sup>Institute of Atmospheric Sciences and Climate (ISAC), National Research  
16 Council (CNR), via P. Gobetti 101, 40129, Bologna Italy

17 <sup>4</sup>Korea Polar Research Institute, 26, SongdoMirae-ro, Yeonsu-Gu, Incheon,  
18 KOREA 406-840

19 <sup>5</sup>Institute for Atmospheric and Earth System Research, University of Helsinki  
20 Helsinki, FI-00014, Finland

21 <sup>6</sup>Finnish Meteorological Institute, FI-00101 Helsinki, Finland

22 <sup>7</sup>Institute of Marine Sciences, Passeig Marítim de la Barceloneta, 37-49. E-  
23 08003, Barcelona, Spain; corresponding author, email: dallosto@icm.csic.es

24

25 <sup>+</sup>Also at: Department of Environmental Sciences/Centre of Excellence in  
26 Environmental Studies, King Abdulaziz University, PO Box 80203, Jeddah,  
27 21589, Saudi Arabia.



1

2 **Abstract**

3

4 The Southern Ocean and Antarctic region currently best represent one of the  
5 few places left on our planet with conditions similar to the preindustrial age.  
6 Currently, climate models have low ability to simulate conditions forming the  
7 aerosol baseline; a major uncertainty comes from the lack of understanding of  
8 aerosol size distributions and their dynamics. Contrasting studies stress that  
9 primary sea-salt aerosol can contribute significantly to the aerosol population,  
10 challenging the concept of climate biogenic regulation by new particle  
11 formation (NPF) from dimethyl sulphide marine emissions.

12 We present a statistical cluster analysis of the physical characteristics of  
13 particle size distributions (PSD) collected at Halley (Antarctica) for the year  
14 2015 (89% data coverage). By applying the Hartigan-Wong k-Means method  
15 we find 8 clusters describing the entire aerosol population. Three clusters  
16 show *pristine* average low particle number concentrations ( $< 121\text{-}179\text{ cm}^{-3}$ )  
17 with three main modes (30 nm, 75-95 nm, 135-160 nm) and represent 57% of  
18 the annual PSD (up to 89-100% during winter, 34-65% during summer based  
19 upon monthly averages). Nucleation and Aitken mode PSD clusters dominate  
20 summer months (Sep-Jan, 59-90%), whereas a clear bimodal distribution (43  
21 and 134 nm, respectively, min Hoppel mode 75 nm) is seen only during the  
22 Dec-Apr period (6-21%). Major findings of the current work include: (1) NPF  
23 and growth events originate from both the sea ice marginal zone and the  
24 Antarctic plateau, strongly suggesting multiple vertical origins, including  
25 marine boundary layer and free troposphere; (2) very low particle number  
26 concentrations are detected for a substantial part of the year (57%), including  
27 summer (34-65%), suggesting that the strong annual aerosol concentration  
28 cycle is driven by a short temporal interval of strong NPF events; (3) a unique  
29 pristine aerosol cluster is seen with a bimodal size distribution (75 nm and 160  
30 nm, respectively), strongly correlating with wind speed and possibly  
31 associated with blowing snow and sea spray sea salt, dominating the winter  
32 aerosol population (34-54%). A brief comparison with two other stations  
33 (Dome C Concordia and King Sejong Station) during the year 2015 (240 days  
34 overlap) shows that the dynamics of aerosol number concentrations and



1 distributions are more complex than the simple sulphate-sea spray binary  
2 combination, and it is likely that an array of additional chemical components  
3 and processes drive the aerosol population. A conceptual illustration is  
4 proposed indicating the various atmospheric processes related to the  
5 Antarctic aerosols, with particular emphasis on the origin of new particle  
6 formation and growth.

7

## 8 **1 Introduction**

9

10 Atmospheric marine aerosol particles contribute substantially to the global  
11 aerosol budget; they can impact the planetary albedo and climate (Reddington  
12 et al., 2017). However, aerosols remain the least understood and constrained  
13 aspect of the climate system (Boucher et al., 2013). Aerosol concentration,  
14 size distribution, chemical composition and dynamic behavior in the  
15 atmosphere play a crucial role in governing radiation transfer. However,  
16 aerosol sources and processes, including critical climate feedback  
17 mechanisms, are still not fully characterized. This is especially true in pristine  
18 environments, where the largest uncertainties are found, mainly due to lack of  
19 understanding of pristine natural sources (Carslaw et al., 2013). Indeed, the  
20 Southern Ocean and the Antarctic region still raises many unanswered  
21 atmospheric science questions. This region has complex interconnected  
22 environmental systems - such as ocean circulation, sea ice, land and snow  
23 cover – which are very sensitive to climate change (Chen et al., 2009).

24 Early research upon Antarctic aerosols was carried out over various part of  
25 the continent and reviewed by Shaw et al. (1988). It was concluded that a  
26 peculiar feature of the Antarctic aerosol system is a very pronounced annual  
27 cycle of the total particle number concentration, with concentrations 20-100  
28 times higher during austral summer than during winter.

29 This seasonal cycle - like a seasonal "pulse" over the summer months  
30 (December, January and February) - seems to be more prominent in the  
31 upper Antarctic plateau than the coastal Antarctic zones, but particle number  
32 concentrations are much higher in coastal Antarctica. One possible origin for  
33 these nuclei could be the Antarctic free troposphere, as suggested by Ito et al.



1 (1993), although this free troposphere to marine boundary layer transport was  
2 considered by no means a definite explanation (Koponen et al., 2002; 2003).  
3 Overall, the aerosol summer maximum concentrations can be largely  
4 explained by new particle formation (NPF) events, as recently reviewed by  
5 Kerminen et al., (2018).

6 The vertical origin of these NPF events is still matter of debate. Some  
7 indications suggesting NPF takes place preferentially in the Antarctic Free  
8 Troposphere (FT): aerosols originate in the upper troposphere, then the  
9 circulation induced by the Antarctic drainage flow (James, 1989) transports  
10 aerosols down to the boundary layer in the Antarctic plateau, with subsequent  
11 transport further to the coast by katabatic winds (Ito et al., 1993; Koponen et  
12 al., 2002; Fiebig et al., 2014; Hara et al., 2011; Järvinen et al., 2013;  
13 Humphries et al., 2016). A recent study found that the Southern Ocean was  
14 the dominant source region for particles observed at Princess Elisabeth (PE)  
15 station, leading to an enhancement in particle number (N), while the Antarctic  
16 continent itself was not acting as a particle source (Herenz et al., 2019).  
17 Further studies also point to boundary layer oceanic sources of NPF events  
18 (Weller et al., 2011; Weller et al., 2015; Weller et al., 2018). Recently, a long  
19 term analysis of the seasonal variability in the physical characteristics of  
20 aerosol particles sampled from the King Sejong Station (located on King  
21 George Island at the top of the Antarctic Peninsula) was reported (Kim et al.,  
22 2017). The CCN concentration during the NPF period increased by  
23 approximately 11 % compared with the background concentration (Kim et al.,  
24 2019). Interestingly, new particle formation events were more frequent in the  
25 air masses that originated from the Bellingshausen Sea than in those that  
26 originated from the Weddell Sea, and it was argued that the taxonomic  
27 composition of phytoplankton could affect the formation of boundary layer new  
28 particles in the Antarctic Ocean (Jang et al., 2019). Dall’Osto et al. (2017)  
29 reported higher N in sea ice-influenced air masses.

30

31 Overall, studies to date suggest that regional NPF events in Antarctica are not  
32 as frequent as those in the Arctic or other natural environments, although the  
33 growth rates are similar (Kerminen et al., 2018). In terms of aerosol size, most  
34 of the ultrafine (<100 nm) particle concentrations have been linked to NPF



1 events, whereas sea salt particles dominate the coarse mode and  
2 accumulation mode ( $>100$  nm). A recent study by Yang et al. (2019), however,  
3 proposes a source for ultrafine sea salt aerosol particle from blowing snow,  
4 dependent on snow salinity. This mechanism could account for the small  
5 particles seen during Antarctic winter at coastal stations.

6  
7 It is interesting to note that the recent, spatially-extensive study of the  
8 concentration of sea-salt aerosol throughout most of the depth of the  
9 troposphere and over a wide range of latitudes (Murphy et al., 2019) reported  
10 a source of sea-salt aerosol over pack ice that is distinct from that over open  
11 water, likely produced by blowing snow over sea ice (Huang et al., 2018;  
12 Giordano et al., 2018; Frey et al., 2019). In recent years, a number of long  
13 term aerosol size distribution datasets have been discussed (Järvinen et al.,  
14 2013; Kim et al., 2019) but these types of datasets are still scarce. The ability  
15 to measure aerosol size distributions at high time resolution allows open  
16 questions to be investigated. The purpose of the present work is to examine  
17 for the first time a one year long (2015) dataset collected at Halley Station.

18  
19 Previous work at the Halley research station reported size-segregated aerosol  
20 samples collected with a cascade impactor at 2 week intervals for a year. Sea  
21 salt was found to be a major component of aerosol throughout the year (60%  
22 of mass) deriving from the sea ice surface rather than open water.  
23 Methanesulphonic Acid (MSA) and non-sea-salt sulphate both peaked in the  
24 summer and were found predominantly in the submicron size range (Rankin  
25 and Wolff, 2003). Observations of new particle formation during a two month  
26 cruise in the Weddell Sea revealed an iodine source (Atkinson et al., 2012).  
27 While no short-term correlation (timescale  $< 2$  days) was found between  
28 particles and iodine compounds in a later study (Roscoe et al., 2015), the  
29 authors highlighted correlations on seasonal timescales. It is also worth  
30 mentioning that a previous Weddell Sea study also found increased new  
31 particle formation in the sea ice zone (Davison et al., 1996), but no clear  
32 correlation between dimethyl sulphide and new particle bursts was found.

33



1 In this paper, we use k-means cluster analysis (Beddows et al., 2009) to  
2 elucidate the properties of the aerosol size distributions collected across the  
3 year 2015 at Halley. A clear advantage of this clustering method over  
4 average size distributions (e.g. monthly, seasonally, etc.) is that specific  
5 aerosol categories of PSD can be compared across different time periods.  
6 While a number of intensive polar field studies have focused on average  
7 monthly datasets, cluster analyses of year long polar and marine particle size  
8 distributions measurements are scarce. Recently, cluster analysis was applied  
9 to Arctic aerosol size distributions taken at Zeppelin Mountain Svalbard;  
10 Dall'Osto et al., 2017a) during an 11-year record (2000–2010) and at Villum  
11 Research Station (Greenland; Dall'Osto et al., 2018b) during a 5-year period  
12 (2012–2016). Both studies showed a striking negative correlation between  
13 sea ice extent and nucleation events, and concluded that NPF are events  
14 linked to biogenic precursors released by open water and melting sea ice  
15 regions, especially during the summer season. Recently, data from three high  
16 Arctic sites (Zeppelin research station, Gruevbadet Observatory, Villum  
17 Research Station at Station Nord) over a 3-year period (2013–2015) were  
18 analysed via clustering analysis, reporting different categories including  
19 pristine low concentrations (12%–14% occurrence), new particle formation  
20 (16%–32%), Aitken (21%–35%) and accumulation (20%–50%) particles  
21 categories (Dall'Osto et al., 2019). To our knowledge, this is the first year-long  
22 Antarctic dataset where cluster analysis has been applied. The objective of  
23 this work is to analyze different types of aerosol size distributions collected  
24 over a whole year of measurements, to elucidate source regions (including  
25 open ocean, land, snow on land, consolidated and marginal sea ice zones),  
26 discuss possible primary and secondary aerosol components, and propose  
27 mechanisms where NPF and growth may take place in the study region.

28  
29  
30  
31  
32  
33



## 1 **2. Methods**

2

### 3 **2.1 Location**

4

5 The measurements reported here were made at the British Antarctic Survey's  
6 Halley VI station (75° 36'S, 26° 11'W), located in coastal Antarctica, on the  
7 floating Brunt Ice Shelf ~20 km from the coast of the Weddell Sea. A variety of  
8 measurements were made from the Clean Air Sector Laboratory (CASLab),  
9 which is located about 1 km south-east of the station (Jones et al., 2008).

10

### 11 **2.2 SMPS and CPC**

12

13 The aerosol size distribution was measured using a TSI Inc. Scanning Mobility  
14 Particle Sizer (SMPS), comprising an Electrostatic Classifier (model 3082), a  
15 Condensation Particle Counter (CPC) model 3775, and a long Differential  
16 Mobility Analyser (DMA, model 3081). The SMPS returned information on  
17 numbers of particles in discrete size bins in the size range 6 nm to 209 nm, at  
18 1-min temporal resolution. A condensation particle counter (CPC, TSI Inc.  
19 model 3010) is routinely run at Halley. It provides a measure of total number  
20 of particles with diameter between 10 nm and ~3 microns. Both instruments  
21 sampled from the CASLab's central, isokinetic, aerosol stack (200 mm i.d.  
22 stainless steel) (see Jones et al. (2008) for details).

23

#### 24 **2.2.1. SMPS K means clustering data analysis**

25

26 Prior to clustering, the SMPS distributions are normalized so that the  
27 Euclidean length of each (treated as a vector) is 1. This ensures that we are  
28 clustering the shape of the distributions irrespective of the magnitude of the  
29 number count within each. The normalized data given then are clustered  
30 using the k-means (method R Core Team (2019)). This partitions the SMPS  
31 distributions (treated as vectors by k-means) into k groups such that the sum  
32 of squares of the distances from these points to the assigned cluster centres



1 is minimized. At the minimum, the cluster centres form the average SMPS  
2 distributions of the individual SMPS distributions assigned to each cluster.  
3  
4 To decide on the number of factors to choose, the Dunn Index and Silhouette  
5 Width were calculated for each factor number. The Dunn Index is the ratio of  
6 the smallest distance between observations not in the same cluster to the  
7 largest intra-cluster distance. The Dunn Index has a value between zero and  
8 infinity, and should be maximized. Similarly, the Silhouette Width analysis is a  
9 measure of how similar the observations are with the cluster they are  
10 assigned to relative to other clusters. Its value ranges from -1 to 1 for each  
11 observation in your data. A value approaching 1 indicates that the elements  
12 within each cluster are identical to each other; a values close to 0 suggest that  
13 there is no clear division between clusters; and a value to -1 suggest that the  
14 observations have been assigned to the wrong cluster. As we increase the  
15 cluster number from 2 up to 30 the Silhouette Width falls from a maximum  
16 value of 0.49 to 0.28 and the Dunn Index increases from a minimum of  $2.9 \times 10^{-3}$   
17 to a maximum  $12.3 \times 10^{-3}$ . As the number of clusters is increased from 2,  
18 the increase in Dunn Index reflects the sequential improvement of the fit as  
19 more clusters are offered to the algorithm to fit the various facets of the data.  
20 In comparison, the Silhouette Width decreases. Although the similarity of the  
21 elements within each cluster will increase, the dissimilarity between each  
22 cluster will decreases and this what drives the Silhouette Width down. When  
23 plotted an optimum of 8 clusters was decided upon (average Silhouette Width  
24 of 0.35 and a Dunn Index of  $4.6 \times 10^{-3}$ ) based upon these two opposing  
25 factors. The first factor being the increase in the fit of the clusters to the  
26 natural clusters within the data with increased cluster number and the second  
27 being the over clustering of the data such that the natural clusters are divided  
28 according to the natural spread of the points within the cluster. This can be  
29 determined by looking for so called 'knees' within the two plots.  
30  
31  
32  
33  
34





1    **2.3 Meteorological and other data**

2

3    **2.4 Air mass trajectories**

4

5    Air mass backtrajectories were calculated using the HYSPLIT4 trajectory  
6    model (Draxler and Hess, 1998) using the NCAR/NCEP 2.5-deg global  
7    reanalysis archive (Kalnay et al., 1996). Trajectories were calculated arriving  
8    at Halley (Lat. 75°34'16"S, Long. 25°28'26"W, 30m above sea level (asl))  
9    every 6 hours (06:00, 12:00, 18:00, 00:00) during the study period. All  
10   calculations were carried out through the Openair trajectory functions in Cran  
11   R (Carslaw and Ropkins 2012). In particular, once calculated, the trajectories  
12   were clustered using the Openair function *trajCluster* using the Euclidean  
13   method. When considering the various cluster numbers, a setting of 6  
14   trajectory clusters were chosen as best describing the air masses arriving at  
15   Halley. Note that metrics similar to the Dunn Index and Silhouette Width were  
16   not needed in this decision. The results of the air mass trajectory calculation  
17   were plotted either as individual, average or raster layer objects (Hijmans  
18   (2019)) drawn on stereographic projections of Antarctica using the *mapproj*  
19   and *maps* package (Becker 2018, Doug McIlroy *et al* 2018).

20

21    **3. Results**

22

23    **3.1 Categorizing Antarctic aerosol size distributions**

24

25    **3.1.1 Average particle number and size resolved concentrations**

26

27    We investigated the seasonal variability in the physical aerosol size  
28    characteristics of particles sampled from Halley VI Station in coastal  
29    Antarctica over the period January to December 2015. A clear maximum at 45  
30    nm and at 145 nm can be seen in the annual average size distribution (Fig. 1).  
31    However, a striking difference can be seen among different seasons: high  
32    concentrations of aerosols at about 40 nm dominate during summer, whereas  
33    larger modes can be observed during winter; with intermediate conditions



1 during spring and autumn. The difference between spring and autumn at  
2  $D > 60$  nm is also interesting, showing much higher concentrations in autumn.  
3 Results are broadly in line with previous results published from the Antarctic  
4 Peninsula (Kim et al., 2017). Total particle number concentrations are  
5 derived from a condensation particle counter (CPC) deployed parallel to the  
6 SMPS (Fig. SI 1), supporting the excellent performance of the SMPS over a  
7 large data coverage (89% of the time during 2015). Minimum concentrations  
8 are found for the month of August ( $47 \pm 10$  cm<sup>-3</sup>) and maximum for January  
9 ( $602 \pm 65$  cm<sup>-3</sup>). These are reflected in the clear seasonal cycles for the total  
10 particle concentration (CN) observed (Fig SI 2). Figure SI 2 (bottom) also  
11 shows daily average concentrations of the  $N_{30 \text{ nm}}$ ,  $N_{30-100 \text{ nm}}$  and  $N_{>100 \text{ nm}}$   
12 integral particle population. The selected cutoffs of 30 and 100 nm are based  
13 on the average shape of the size distribution (Figure 1). It is interesting that  
14 whereas the absolute concentrations are remarkably different, the relative  
15 percentages of the three aerosol populations do not differ much across  
16 different months, on average  $21 \pm 9\%$ ,  $54 \pm 7\%$  and  $25 \pm 8\%$  for the  $N_{30 \text{ nm}}$ ,  $N_{30-100}$   
17  $\text{nm}$  and  $N_{>100 \text{ nm}}$ , respectively. Ultrafine particles dominate summer  
18 concentrations, but are - relative to total - a dominating fraction also during  
19 winter.

20

### 21 **3.1.2 K-means SMPS cluster analysis**

22

23 K-means cluster analysis of particle number size distributions was performed  
24 using 5,664 hourly distributions collected over the year of 2015. Our clustering  
25 analysis led to an optimum number of eight categories of aerosol number size  
26 distributions. The corresponding average daily aerosol number size  
27 distributions are shown in Figure 2a, whereas the annual seasonality is shown  
28 in Figure 2b. Here, we refer to ultrafine as particles with diameters between 6  
29 and 210 nm. Three categories were characterized by very low particle number  
30 concentrations ( $< 200$  particles cm<sup>-3</sup>), and described by their different aerosol  
31 modes (plotted and size resolved in Fig. 3), specifically:

32

33 - "*Pristine\_30*" ultrafine. Occurring annually 19% of the time (min-max 0-55%  
34 based on monthly averages), this aerosol category ( $N_{\text{CPC}} 179 \pm 30$  cm<sup>-3</sup>) shows



1 two main peaks at 30 nm and 95 nm (Fig. 3, Fig. SI 3). The maximum in  
2 occurrence is seen for the months of September (47%) and May (55%).

3  
4 - "*Pristine\_75*" ultrafine. Occurring annually 29% of the time (min-max 0-61%  
5 based on monthly averages), this aerosol category ( $N_{\text{CPC}} 157 \pm 25 \text{ cm}^{-3}$ ) shows  
6 two main peaks at 70 nm and 130 nm (Fig. 3, Fig. SI 3). The occurrence is  
7 scattered across all year except during spring months (Sept/Oct).

8  
9 - "*Pristine\_160*" ultrafine. Occurring annually 9% of the time (min-max 0-52%  
10 based on monthly averages), this aerosol category ( $N_{\text{CPC}} 121 \pm 40 \text{ cm}^{-3}$ ) shows  
11 two main peaks at 70 nm and 160 nm (Fig. 3, Fig. SI 3). The maximum in  
12 occurrence is seen for the winter months of June (41%) and July (52%).

13  
14 These three pristine aerosol cluster types describe up to 57% of the aerosol  
15 population, and mainly dominate the aerosol population during cold months  
16 (73%-100% for Apr-Aug.) Other aerosol categories possessing higher particle  
17 concentrations include:

18  
19 - "*Nucleation*" ultrafine. Occurring annually 3% of the time (min-max 0-11%  
20 based on monthly averages), this aerosol category ( $N_{\text{CPC}} 620 \pm 220 \text{ cm}^{-3}$ )  
21 shows a main nucleation peak at 15 nm detected during summer months (Fig.  
22 2 a, b). Figure SI3d shows the evolution of the aerosol number size  
23 distributions starting at about noon and peaking at about 18:00; overall 95% of  
24 these events were detected during daylight. The name of this category - which  
25 will be used below to represent new particle formation events - stands for  
26 continuous gas-to-particle growth occurring after the particle nucleation event,  
27 although these nucleation events - detected at about 7-10 nm - must have  
28 originated away from the Halley station.

29  
30 - "*Bursting*" ultrafine. Occurring annually 9% of the time (min-max 0-37%  
31 based on monthly averages), this aerosol category ( $N_{\text{CPC}} 602 \pm 120 \text{ cm}^{-3}$ )  
32 shows a main nucleation peak at 27 nm detected during summer months (Fig.  
33 2a, b). Fig. SI3e suggests these aerosols are similar to the *Nucleation* cluster,



1 although these new particle formation events are already in the growth  
2 process almost reaching 30 nm on average.

3  
4 Clusters *Nucleation* and *Bursting* are seen during summer months and  
5 September-October, contributing up to 44% of the total aerosol population  
6 during the months of September and January (Fig. SI4b, d). Following  
7 terminology developed in previous work (Dall’Osto et al., 2017, 2018) the  
8 remaining aerosol clusters can be classified as followed:

9  
10 - "*Nascent*" ultrafine. This category occurs annually 10% of the time, with a  
11 strong seasonal trend peaking during summer (October-December, 10-39%)  
12 and with a broad Aitken mode centred at about 38 nm (Fig.2) without showing  
13 a clear diurnal pattern (Fig. SI3f). The name of this category emerges from  
14 growing ultrafine aerosol particles which may result from an array of different  
15 primary and secondary aerosol processes.

16  
17 - "*Aitken*" ultrafine. This category occurs annually 15% of the time, with a  
18 strong seasonal trend peaking during summer (Oct-Dec, 32-63%, Fig. 2b) and  
19 - similar to the *Nascent* cluster - a broad Aitken mode centred at about 50 nm  
20 (Fig 2a) without showing a clear diurnal pattern (Fig. SI 3h).

21  
22 - "*Bimodal*" ultrafine. Occurring annually 5% (min-max 0-21%) of the time, this  
23 unique category shows a strongly bimodal size distribution (43nm and 134nm,  
24 with a small nucleation mode at 16 nm, Fig. 2 a), it occurs during the period  
25 Dec-Apr (7-21%) and parallels previously reported bimodal aged Antarctic  
26 distributions (Ito et al., 1993). The minimum of the Hoppel mode is seen at 70  
27 nm.

28  
29 In summary, our method allows apportionment of the Antarctic aerosol  
30 observed at Halley research station into eight categories describing the whole  
31 aerosol population. In the following sections, emphasis is given to  
32 understanding the origin and processes driving Antarctic aerosol formation.

33



1 **3.2 Association of PSD with meteorological, physical and chemical**  
2 **parameters**

3  
4 The main ground-level meteorological observations from Halley for the year  
5 2015 are temporally averaged over the periods of occurrence of the different  
6 aerosol categories (Fig SI 5). Higher average wind speeds (WS,  $7.2 \pm 2 \text{ m s}^{-1}$ )  
7 were encountered for the pristine aerosol clusters relative to the remaining  
8 five ( $3.2 \pm 2 \text{ m s}^{-1}$ ); cluster *pristine\_160* shows the highest WS ( $8.5 \pm 3 \text{ m s}^{-1}$ ),  
9 suggesting the larger mode may be due to a primary aerosol component,  
10 further discussed in Section 4. Little variation in atmospheric pressure was  
11 found among the eight aerosol clusters. By contrast, *Nucleation* and *Bursting*  
12 clusters were found in driest (Relative Humidity RH,  $48 \pm 5\%$ ) and coldest (T -  
13  $17 \pm 0.2 \text{ }^\circ\text{C}$ ) weather among all clusters, supporting the fact that NPF takes  
14 place preferentially at low RH (Laaksonen et al.; 2009; Hamed et al. 2011).  
15 Vertical profiles of meteorological data are available for most days in 2015,  
16 and complement local ground-level measurements. Fig. SI6a-b show driest  
17 and coldest conditions for clusters *Bursting* and *Nucleation*. By contrast,  
18 warmest and wettest conditions occur for the *Bimodal* category. A large  
19 difference is also seen in the wind speed vertical profiles (Fig. SI 6c), which  
20 are strongest for cluster *pristine\_160*, and a clear inversion is seen during the  
21 *bimodal* cluster days. Concurrent ozone gas measurements (Fig. SI 5) show  
22 lowest values for the cluster *bimodal* ( $18 \pm 3 \text{ ppb}$ ), moderate for ultrafine  
23 dominating clusters ( $24 \pm 8 \text{ ppb}$ ), and higher values for pristine clusters ( $29 \pm 5$   
24  $\text{ppb}$ ).

25  
26 **3.3 Elucidating source regions by association of PSD clusters with air**  
27 **mass back trajectories**

28  
29 Throughout the studied period, hourly 120 h back trajectories were calculated  
30 using the HYSPLIT4 model (Draxler and Hess, 1998). Figure 4 shows the  
31 results of the air mass back trajectories calculated for Halley throughout 2015,  
32 showing six main clusters. Broadly, two air trajectory clusters were associated  
33 with anticyclonic conditions (clusters 2 and 6, up to 33.6% of air masses);  
34 three clusters were associated with air masses coming from the East Antarctic



1 Plateau (clusters 3, 4, 5, up to 57.2% of air masses); and one unique air  
2 trajectory cluster was found associated with air masses originating within the  
3 Weddell Sea (cluster 1, 9%). Fig. SI7 shows the six air mass back trajectory  
4 clusters and the average height of the trajectories up to 120 hours before  
5 arrival at Halley. While clusters 2-6 show their origin over the Antarctic plateau,  
6 cluster 1 shows average altitudes lower than 1000m, close to the height of the  
7 mixed layer (Fig. SI 7). On the basis of Figure SI7, it looks rather similar to the  
8 other air mass types with the air only entering the boundary layer for the last  
9 ~15 hours of the trajectory. One striking difference is found when these air  
10 mass back trajectory clusters are compared temporally among the aerosol  
11 categories (Figure 5).

12 A key conclusion of this study is that most aerosol categories (excluding  
13 cluster *Nucleation*) are associated with air masses arriving with Eastern winds  
14 from the Antarctic plateau (East short, East long, 56-76% of the time).  
15 Anticyclones also seem to be a predominant air mass type (17-42%). At  
16 Halley, air mass back trajectories that have travelled over the sea/sea ice  
17 zone, play only a minor overall role in terms of annual average air mass  
18 trajectories (10-15%). In a further analysis, we obtained information on how  
19 far each air mass travelled (total travel time 60 h) over zones distinguished by  
20 their surface characteristics, namely snow, sea ice and open water for each  
21 one of the different aerosol categories presented (see methods). Fig. 5a  
22 shows that category *Nucleation* is the one most associated with sea ice (27%  
23 of the time). It is important to stress that the *Nucleation* category has its air  
24 mass back trajectories mainly travelling over land (63%). However - relative to  
25 the other clusters - it is the most affected by air masses which had travelled  
26 over the Weddell Sea (27%), most of which is open pack ice (ratio open pack /  
27 consolidated sea ice of 0.6, Fig. 5b). This is an important conclusion of this  
28 work, pointing out that at least two source regions of new particle formation  
29 exist in the Antarctic. It is interesting to note also that the *Bursting* category  
30 has a large ratio of open pack / consolidated sea ice (Fig 5b), confirming  
31 marginal sea ice zones may be a strong source of biogenic gases responsible  
32 for new particle formation.

33 By examining the air mass trajectory heights, we also show that during the 5  
34 days prior to sampling, the sampled air from the Weddell Sea was remarkably



1 different from the other air mass types (Fig. SI 7); it had travelled within the  
2 marine boundary layer, with no intrusion from the free troposphere. Our  
3 results strongly suggest the nucleating events originated within the boundary  
4 layer, likely from gaseous precursors associated with sea ice emissions.

5

6

## 7 **4. Discussion**

8

### 9 **4.1 Origin and sources of Antarctic aerosol**

10

11 The purpose of this study was to analyze a year-long (throughout 2015) set of  
12 observations of Antarctic aerosol number size distributions to gain a better  
13 understanding of those processes which control Antarctic aerosol properties.  
14 In a pristine environment like Antarctica and its surrounding ocean, where the  
15 atmosphere is thought to still resemble that of preindustrial Earth (Hamilton et  
16 al., 2014), missing aerosol sources must reflect overlooked natural processes.  
17 Uncertainties for modeling aerosol-cloud interactions and cloud radiative  
18 forcing arise from a poor source apportionment of aerosols and their size  
19 distributions (Carslaw et al 2013).

20 Broadly, marine particles in the nanometer size range originate from gas-to-  
21 particle secondary processes, whereas those in super-micron sizes are  
22 predominantly composed of primary sea-spray (O'Dowd et al., 1997).  
23 However, the accumulation mode (broadly composed of intermediate particle  
24 sizes of 50 –500 nm) is composed of a complex mixture of both secondary  
25 and primary particles. The relative roles of secondary aerosols produced from  
26 biogenic sulfur versus primary sea-spray aerosols in regulating cloud  
27 properties and amounts above the Southern Ocean is still a matter of debate  
28 (Meskhidze and Nenes, 2006; Korhonen et al., 2008; Quinn and Bates, 2011;  
29 Mc Coy et al., 2015; Gras and Keywood, 2017; Fossum et al., 2018). First  
30 observations of organic carbon (OC) in size-segregated aerosol samples  
31 collected at a coastal site in the Weddell Sea (Virkkula et al., 2006) showed  
32 that MSA represented only a few % of the total OC in the submicron fraction;  
33 recent studies demonstrate that sea bird colonies are also important sources



1 of organic compounds locally (Schmale et al., 2013; Liu et al., 2018) and from  
2 seasonal ice microbiota (Dall'Osto et al., 2017). The overall balance between  
3 secondary aerosol formation versus primary particle formation from sea spray  
4 still needs to be determined and is a pressing open question.

5  
6 A key result of this study is that for 59% of the year (89-100% during winter  
7 JJA; 10-50% during spring SON; 34-65% during summer DJF; 48-91% during  
8 autumn MAM), aerosol size distributions were characterized by very low  
9 particle number concentrations ( $< 121\text{-}179\text{ cm}^{-3}$ ). It is often assumed that a  
10 strong annual cycle of particle number concentrations is mainly driven by  
11 summer new particle formation events (Shaw, 1988; Ito et al., 1993; Kerminen  
12 et al., 2018). However, at Halley during summer 2015, 34-65% of the time low  
13 particle number concentrations of unknown origin dominate the overall  
14 temporal variation. Unique bimodal size distributions are seen in December-  
15 April, where a clear bimodal distribution is seen for 7-21% of the time (peaking  
16 in March, 21%), and likely related to cloud processing (Hoppel et al., 1994).

17 In the following sub-sections we discuss our results in the light of recent  
18 studies focusing on Antarctic aerosol source apportionment. The majority of  
19 the studies report primary and secondary components in term of mass, which  
20 should not be confused with particle number concentration.

21

#### 22 **4.1.1 Primary Antarctic aerosol**

23

24 Sea spray is almost always reported as the main source of supermicron ( $>1$   
25  $\mu\text{m}$ ) aerosols in marine areas, including the Southern Ocean and Antarctica  
26 (Quinn et al., 2015; Bertram et al., 2018). However, models of global sea-salt  
27 distribution have frequently underestimated concentrations at polar locations  
28 (Gong et al., 2002). Rankin and Wolff (2003) suggested the Antarctic sea ice  
29 zone was a more important source of sea salt aerosol, during the winter  
30 months, than the open ocean. In particular, they proposed brine and frost  
31 flowers on the surface of newly forming sea ice as the dominant source, a  
32 hypothesis supported by other studies (e.g. Udisti et al., 2012). The results  
33 presented here suggest that, in coastal Antarctica, aerosol composition is a  
34 strong function of wind speed and that the mechanisms determining aerosol





1 composition are likely linked to blowing snow (Giordano et al., 2019; Yang et  
2 al., 2019; Frey et al., 2019). We note that Legrand et al. (2017a) suggested  
3 that on average, the sea-ice and open-ocean emissions equally contribute to  
4 sea-salt aerosol load of the inland Antarctic atmosphere.

5 Averaged across the year, we found a very clear aerosol size distribution with  
6 the largest detected mode at ~160 nm, pointing to a primary - likely sea spray  
7 - source, which was detected during periods of strong winds. However, it is  
8 also possible that in size range the dominating constituent is sulphate (Teinilä  
9 et al., 2014), further studies are needed to apportion this mode correctly. This  
10 aerosol category type occurs very frequently during winter months (JJ, 33-  
11 52%), but not during the other months (0-14%). Gras and Keywood (2017)  
12 showed, using data from Cape Grim, that wind-generated coarse-mode sea  
13 salt is an important CCN component year round and from autumn through to  
14 mid-spring is the second most important component, contributing around 36%  
15 to observed CCN; these measurements were taken in the Southern Ocean  
16 marine boundary layer.

17 Marine primary organic aerosol (POA) is often associated with sea-spray, but  
18 recent studies indicate that a fine mode (usually <200 nm) can have a size  
19 distribution that is independent from sea-salt (externally mixed), whereas  
20 supermicron marine aerosols are more likely to be internally mixed with sea-  
21 salt (Gantt and Meskhidze, 2013). McCoy et al. (2015) reported observational  
22 data indicating a significant spatial correlation between regions of elevated  
23 Chl-a and particle number concentrations across the Southern Ocean, and  
24 showed that modeled organic mass fraction and sulphate explains  $53 \pm 22\%$   
25 of the spatial variability in observed particle concentration. Our study cannot  
26 apportion any aerosol related to primary organic aerosol, given the lack of  
27 chemical measurements carried out during 2015 at Halley research station. It  
28 is possible that part of the broad mode at 90 nm of the Pristine\_90 category  
29 contain a fraction of primary marine organic aerosols, but the relative  
30 importance cannot be quantified in this study. Interestingly, open ocean  
31 aerosol measurements collected over the Southern Ocean (43°S–70°S) and  
32 the Amundsen Sea (70°S–75°S) were recently reported by Jung et al. (2019).  
33 During the cruise, Water Insoluble Organic Components (WIOC) was the



1 dominant Organic Carbon (OC) species in both the Southern Ocean and the  
2 Amundsen Sea, accounting for 75% and 73% of total aerosol organic carbon,  
3 respectively. The WIOC concentrations were found to correlate with the  
4 relative biomass of a specific phytoplankton species (*P. Antarctica*), producing  
5 extracellular polysaccharide mucus and strongly affecting the atmospheric  
6 WIOC concentration in the Amundsen Sea (Jung et al., 2019).

7

#### 8 **4.1.2 Secondary Antarctic aerosol**

9

10 Our results show that two sub 30 nm aerosol categories (*Nucleation* and  
11 *Bursting*, 12% in total) and two Aitken 30-60 nm aerosol categories (*Nascent*  
12 and *Aitken*, 25%) account for up to 37% of the PSD detected during at Halley  
13 the year 2015. Our results point to secondary aerosol processes driving the  
14 aerosol population during five months of the year (Sep-Jan, 48-90%), where  
15 aerosol particle number concentrations are on average 3-4 higher than the  
16 Antarctic aerosol baseline. Our study strongly suggests that new particle  
17 formation may have at least two contrasting sources. The former is related to  
18 sea ice marginal zones formed in the marine boundary layer. The latter is  
19 related to air masses arriving from the Antarctic plateau, possibly having a  
20 free troposphere origin.

21 The biogenic precursors responsible for the new particle formation are not  
22 known. Charlson et al. (1987) postulated the CLAW hypothesis - the most  
23 significant source of CCN in the marine environment is non-sea-salt sulfate  
24 derived from atmospheric oxidation of dimethylsulfide (DMS); however  
25 measurements able to provide information on where individual particles come  
26 from are still limited (O'Dowd et al., 1997b; Quinn and Bates, 2011; Sanchez  
27 et al., 2018). A previous ship-borne field campaign in the Weddell Sea found  
28 increased new particle formation in the sea ice zone of the Weddell Sea  
29 (Davison et al., 1996), but no clear correlation to the dimethyl sulphide that  
30 was then assumed to control new particle bursts. A smaller mode radius  
31 associated with polar aerosol (relative to marine Southern ocean aerosol) was  
32 found associated with less cloud cover, and consequently less cloud  
33 processing, over the continent and pack ice regions. During the cruise, new  
34 particle formation observed over the Weddell Sea, resulted from boundary



1 layer nucleation bursts rather than tropospheric entrainment. Brooks and  
2 Thornton (2018) argued that additional modeling studies are still needed that  
3 address contributions from both secondary DMS-derived aerosols and primary  
4 organic aerosols as CCNs on realistic timescales; although the occurrence of  
5 a “seasonal CLAW” in remote marine atmospheres is becoming plausible  
6 (Vallina and Simó, 2007; Quinn et al., 2017; Sanchez et al., 2018).

7  
8 Satellite (Schonhardt et al., 2008) and on-site measurements (Saiz-Lopez et  
9 al., 2007; Atkinson et al., 2012) showed that the Weddell Sea is an iodine  
10 hotspot; however there was no short-term correlation between IO and particle  
11 concentration found (Roscoe et al., 2015). Using an unprecedented suite of  
12 instruments, Jokinen et al. (2018) showed that ion-induced nucleation of  
13 sulfuric acid and ammonia, followed by sulfuric acid–driven growth, is the  
14 predominant mechanism for NPF and growth in eastern Antarctica a few  
15 hundred kilometers from the coast (Finnish Antarctic research station (Aboa)  
16 is located at the Queen Maud land, Eastern Antarctica; Jokinen et al., 2018).  
17 Some ion clusters contained iodic acid, but its concentration was very small,  
18 and no pure iodic acid or iodine oxide clusters were detected (Sipila et al.,  
19 2016). Finally, some organic oxidation products from land melt ponds have  
20 also been suggested (Kyro et al., 2013) as a potential source for condensable  
21 vapor, although this may be a confined and minor source (Weller et al., 2018).  
22 Other measurements of new particle formation and growth were governed by  
23 the availability of other yet unidentified gaseous precursors, most probably low  
24 volatile organic compounds of marine origin (Weller et al., 2015; 2018).

25

#### 26 **4.2 Implication for climate and conclusion**

27

28 A strong annual cycle of total particle number concentration is a prominent  
29 characteristic of the Antarctic aerosol system, with the austral summer  
30 concentration being up to 20-100 times greater than during the winter (Shaw  
31 1988, Gras 1993, Ito 1993, Hara et al 2011, Weller et al 2011, Järvinen et al  
32 2013, Fiebig et al 2014, Kim et al 2017). These summer particle number  
33 concentration maxima are largely explained by NPF taking place in the



1 Antarctic atmosphere. However, these seasonal cycles are more pronounced  
2 at monitoring sites situated on the upper plateau of Antarctica than at the  
3 coastal Antarctic sites. It is worth to keep in mind that these cycles could also  
4 be more pronounced because in coastal regions in winter, sea salt aerosol  
5 has a relatively larger source. i.e. the amplitude of the seasonal is driven both  
6 by what is going on in winter as well as summer. Nevertheless, overall much  
7 higher particle number concentrations have long been reported in coastal  
8 Antarctica relative to the plateau. The vertical location of Antarctic NPF has  
9 not been well quantified; there are some indications that NPF takes place  
10 preferentially in the Antarctic Free Troposphere (FT) rather than in the  
11 Boundary Layer (BL) (Koponen et al 2002, Hara et al 2011, Humphries et al  
12 2016), whereas other studies shows opposite trends (Kim et al., 2017, Weller  
13 et al., 2011; 2013; 2018). A study conducted on the upper plateau of  
14 Antarctica demonstrates that also wintertime regional NPF is possible in this  
15 environment (Järvinen et al 2013). Very low particle growth rates (between  
16 about 0.1 and 1 nm h<sup>-1</sup>) were reported in Antarctica (Park et al 2004, Weller et  
17 al 2015).

18  
19 We obtained data from Dome C and King Sejong (KS) Station for the period  
20 May-December 2015, and compared them with Halley (H). Data are shown in  
21 Fig. 6 where seasonal mean aerosol size distributions measured  
22 simultaneously at three different sites are reported for (a) May-December  
23 2015 (8 months in total); (b) Spring (September, October, November, 3  
24 months in total); (c) Summer (December, 1 month in total) and (d) Winter  
25 (June, July, August, 3 months in total, a map of the three stations considered  
26 is shown in Figure 7. Overall, much higher concentrations are seen at the  
27 coastal Antarctic sites (H, KS stations) relative to Dome C station (Fig. 6a).  
28 Two broad modes at about 30-50 nm and at about 110-160 nm can be seen  
29 for the coastal stations, whereas a smaller single mode at 60 nm is seen for  
30 the Dome C station. When three seasons are compared, very different  
31 features can be seen. During spring (Fig. 6b), both Aitken and accumulation  
32 modes dominate the coastal sites, whereas a strong single mode is seen in  
33 the Dome C site. By contrast, during summer (Fig. 6c), much stronger  
34 nucleation and Aitken modes are seen at the coastal sites, likely due to NPF



1 taking place during summer time. The smaller nucleation mode size detected  
2 in the Antarctic peninsula (King Sejong Station) relative to the one seen at  
3 Halley may suggest a more local source of NPF in the Antarctic peninsula,  
4 including open water, coastal macroalgae, and bird colonies. The average  
5 size distributions during winter (Fig. 6d) again show marked differences  
6 among the three different monitoring sites. Halley stations shows the largest  
7 aerosol modes (about 100 nm and 160 nm), whereas smaller modes can be  
8 seen at the other two sites. Overall, Fig. 6 serves to stress that the aerosol  
9 population in Antarctica - an environment often considered homogenous and  
10 simple to study - is different in different geographical regions, and very likely a  
11 number of different processes and sources affect the aerosol population at  
12 different times of the year. Ito et al. (1993) presented a conceptual diagram,  
13 where different aerosol size distributions were seen, and a main NPF mode  
14 was associated with the free troposphere and transported by katabatic winds.  
15 Korhonen et al. (2008) also estimated that over 90% of the non-sea spray  
16 CCN were generated above the boundary layer by nucleation of sulfuric acid  
17 aerosol in the free troposphere. Our results point to sea ice regions and open  
18 ocean water being a source not only of gaseous precursors, but also of new  
19 particle formation, which then can growth once lifted in the free troposphere  
20 (Fig. 8), and then larger modes are brought down again by the Antarctic  
21 Drainage flow (James, 1989). The relative importance of free troposphere  
22 versus boundary layer nucleation is not known at this stage, but this study  
23 shows that the latter is seen, and the former is likely to happen and contribute  
24 to the Aitken mode detected from the Antarctic plateau. Sea ice regions  
25 (mainly via secondary processes, but also to a lesser degree via sea spray  
26 and blowing snow) may control the CCN production, both regulating the first  
27 stage of nucleation events and providing gaseous precursors, and slowly  
28 growing nucleated particles with transport in the upper troposphere.

29  
30 These results are in line with previous studies in polar areas. First, Dall'Osto  
31 et al (2017) suggested that the microbiota of sea ice and sea ice-influenced  
32 ocean were a significant source of atmospheric nucleating particles  
33 concentrations ( $N_{1-3nm}$ ). Second, within two different Arctic locations, across  
34 large temporal scales (2000-2016) new particle formation was associated with



1 air mass back trajectories passing over open water and melting sea ice  
2 regions, also pointing to marine biological activities within the open leads in  
3 the pack ice and/or along the melting marginal sea ice zone (MIZ) being  
4 responsible for such events (Dall’Osto et al., 2017b, Dall’Osto et al., 2018).  
5 Our data from Halley, and the brief intercomparison with two other stations,  
6 suggest that the size distributions of Antarctic submicron aerosols may have  
7 been oversimplified in the past (Ito et al., 1993); and complex interactions  
8 between multiple ecosystems, coupled with different atmospheric circulation,  
9 result in very different aerosol size distributions populating the Southern  
10 Hemisphere.

11  
12  
13

#### 14 **Acknowledgements**

15 The authors are grateful to the overwintering staff at Halley station who  
16 carried out the suite of measurements presented here. This work was funded  
17 by the Natural Environment Research Council as part of the British Antarctic  
18 Survey’s research programme “Polar Science for Planet Earth”. The study  
19 was further supported by the Spanish Ministry of Economy through project PI-  
20 ICE (CTM 2017–89117-R) and the Ramon y Cajal fellowship (RYC-2012-  
21 11922). The National Centre for Atmospheric Science NCAS Birmingham  
22 group is funded by the UK Natural Environment Research Council. We thank  
23 Dr. Pasi aalto (Institute for Atmospheric and Earth System Research,  
24 University of Helsinki), for providing DMPSdata of 2015 for intercomparison  
25 with data taken at Halley Station, similar data were discussed in details  
26 elsewhere (Järvinen et al., 2013; Kim et al., 2017) . AV as supported by the  
27 Academy of Finland’s Centre of Excellence program (Centre of Excellence in  
28 Atmospheric Science – From Molecular and Biological processes to The  
29 Global Climate, project no. 272041). KS station SMPS measurement was  
30 supported by KOPRI project (PE19010).

31  
32  
33  
34  
35



1  
2  
3  
4  
5  
6  
7  
8  
9  
10  
11  
12  
13  
14  
15  
16  
17  
18  
19  
20  
21  
22  
23  
24  
25  
26  
27  
28  
29  
30  
31  
32  
33  
34  
35  
36  
37  
38  
39  
40  
41  
42  
43  
44  
45  
46  
47  
48  
49

## References

Asmi, E., Frey, A., Virkkula, A., Ehn, M., Manninen, H., Timonen, H., Tolonen-Kivimäki, O., Aurela, M., Hillamo, R., and Kulmala, M.: Hygroscopicity and chemical composition of Antarctic sub-micrometre aerosol particles and observations of new particle formation, *Atmos. Chem. Phys.*, 10, 4253–4271, <https://doi.org/10.5194/acp-10-4253-2010>, 2010.

Atkinson, H. M., R.-J. Huang, R. Chance, H. K. Roscoe, C. Hughes, B. Avison, A. Schönhardt, A. S. Mahajan, A. Saiz-Lopez, and P. S. Liss (2012), Iodine emissions from the sea ice of the Weddell Sea, *Atmos. Chem. Phys.*, 12, 11,229–11,244, doi:10.5194/acp-12-11229-2012.

Becagli, S., Scarchilli, C., Traversi, R., Dayan, U., Severi, M., Frosini, D., Vitale, V., Mazzola, M., Lupi, A., Nava, S., and Udisti, R.: Study of present-day sources and transport processes affecting oxidised sulphur compounds in atmospheric aerosols at Dome C (Antarctica) from year-round sampling campaigns, *Atmos. Environ.*, 52, 98–108, <https://doi.org/10.1016/j.atmosenv.2011.07.053>, 2012.

Beddows, D. C. S., Dall'Osto, M., and Harrison, R. M.: Cluster Analysis of Rural, Urban and Curbside Atmospheric Particle Size Data, *Environ. Sci. Technol.*, 43, 4694–4700, 2009.

Beddows, D. C. S., Dall'Osto, M., Harrison, R. M., Kulmala, M., Asmi, A., Wiedensohler, A., Laj, P., Fjaeraa, A. M., Sellegri, K., Birmili, W., Bukowiecki, N., Weingartner, E., Baltensperger, U., Zdimal, V., Zikova, N., Putaud, J.-P., Marinoni, A., Tunved, P., Hansson, H.-C., Fiebig, M., Kivekäs, N., Swietlicki, E., Lihavainen, H., Asmi, E., Ulevicius, V., Aalto, P. P., Mihalopoulos, N., Kalivitis, N., Kalapov, I., Kiss, G., de Leeuw, G., Henzing, B., O'Dowd, C., Jennings, S. G., Flentje, H., Meinhardt, F., Ries, L., Denier van der Gon, H. A. C., and Visschedijk, A. J. H.: Variations in tropospheric submicron particle size distributions across the European continent 2008–2009, *Atmos. Chem. Phys.*, 14, 4327–4348, <https://doi.org/10.5194/acp-14-4327-2014>, 2014.

Bertram, T.H.; Cochran, R.E.; Grassian, V.H.; Stone, E.A. Sea spray aerosol chemical composition: Elemental and molecular mimics for laboratory studies of heterogeneous and multiphase reactions. *Chem. Soc. Rev.* 2018, 47, 2374–2400

Boucher, O., Randall, D., Artaxo, P., Bretherton, C., Feingold, G., Forster, P., Kerminen, V. M., Kondo, Y., Liao, H., Lohmann, U., Rasch, P., Satheesh, S., Sherwood, S., Stevens, B., and Zhang, X.: Clouds and aerosols, in: *Climate change 2013: the physical science basis. Contribution of working group I to the fifth assessment report of the intergovernmental panel on climate change,*





- 1 edited by: Stocker, T. F., Qin, D., Plattner, G. K., Tignor, M., Allen, S.,  
2 Boschung, J., Nauels, A., Xia, Y., Bex, V., and Midgley, P., chap. 7,  
3 Cambridge University Press, Cambridge, 2013.  
4  
5 Brooks, S. D. and Thornton, D. C. O.: Marine Aerosols and Clouds,  
6 *Annu. Rev. Mar. Sci.*, 10, 289–313, 2018  
7  
8 Carslaw, K. S., Lee, L. A., Reddington, C. L., Pringle, K. J., Rap, A., Forster, P.  
9 M., Mann, G. W., Spracklen, D. V., Woodhouse, M. T., Regayre, L. A., and  
10 Pierce, J. R.: Large contribution of natural aerosols to uncertainty in indirect  
11 forcing,  
12  
13 Carslaw, D. C. and K. Ropkins, (2012) openair --- an R package for air quality  
14 data analysis. *Environmental Modelling & Software*. Volume 27-28, 52-61.  
15 10.1016/j.envsoft.2011.09.008  
16  
17 Charlson, R. J., Lovelock, J. E., Andreae, M. O., and Warren, S. G.: Oceanic  
18 Phytoplankton, Atmospheric Sulfur, Cloud Albedo and Climate, *Nature*, 326,  
19 655–661, <https://doi.org/10.1038/326655a0>, 1987.  
20  
21 Chen, J. L., C. R. Wilson, D. Blankenship, and B. D. Tapley  
22 (2009), Accelerated Antarctic ice loss from satellite gravity  
23 measurements, *Nat. Geosci.*, 2, 859–862, doi:10.1038/ngeo694.  
24  
25 Dall'Osto, M., Monahan, C., Greaney, R., Beddows, D. C. S., Harrison, R. M.,  
26 Ceburnis, D., and O'Dowd, C. D.: A statistical analysis of North East Atlantic  
27 (submicron) aerosol size distributions, *Atmos. Chem. Phys.*, 11, 12567–12578,  
28 <https://doi.org/10.5194/acp-11-12567-2011>, 2011.  
29  
30 Dall'Osto, M., Beddows, D. C. S., Tunved, P., Krejci, R., Ström, J., Hansson,  
31 H.-C., Yoon, Y. J., Park, K.-T., Becagli, S., Udisti, R., Onasch, T., O'Dowd, C.  
32 D., Simó, R., and Harrison, R. M.: Arctic sea ice melt leads to atmospheric new  
33 particle formation, *Sci. Rep.*, 7, 3318, [https://doi.org/10.1038/s41598-017-](https://doi.org/10.1038/s41598-017-03328-1)  
34 [03328-1](https://doi.org/10.1038/s41598-017-03328-1), 2017a  
35  
36 Dall'Osto, M., Ovadnevaite, J., Paglione, M., Beddows, D. C. S., Ceburnis, D.,  
37 Cree, C., Cortes, P., Zamanillo, M., Nunes, S. O., Perez, G. L., Ortega-  
38 Retuerta, E., Emelianov, M., Vaque, D., Marrase, C., Estrada, M., Sala, M. M.,  
39 Vidal, M., Fitzsimons, M. F., Beale, R., Airs, R., Rinaldi, M., Decesari, S.,  
40 Facchini, M. C., Harrison, R. M., O'Dowd, C., and Simo, R.: Antarctic sea  
41 ice region as a source of biogenic organic nitrogen in aerosols, *Scientific*  
42 *Reports*, 7, 6047, [https://doi.org/10.1038/s41598-017-](https://doi.org/10.1038/s41598-017-06188-x)  
43 [06188-x](https://doi.org/10.1038/s41598-017-06188-x), 2017b  
44  
45  
46 Dall'Osto, M., Beddows, D. C. S., Asmi, A., Poulain, L., Hao, L., Freney, E.,  
47 Allan, J. D., Canagaratna, M., Crippa, M., Bianchi, F., de Leeuw, G., Eriksson,  
48 A., Swietlicki, E., Hansson, H. C., Henzing, J. S., Granier, C., Zemanekova, K.,  
49 Laj, P., Onasch, T., Prevot, A., Putaud, J. P., Sellegri, K., Vidal, M., Virtanen,





- 1 A., Simo, R., Worsnop, D., O'Dowd, C., Kulmala, M., and Harrison, R. M.:  
2 Novel insights on new particle formation derived from a paneuropean  
3 observing system, *Sci. Rep.*, 8, 1482, [https://doi.org/10.1038/s41598-017-](https://doi.org/10.1038/s41598-017-17343-9)  
4 [17343-9](https://doi.org/10.1038/s41598-017-17343-9), 2018a.  
5  
6 Dall'Osto, M., Geels, C., Beddows, D.C.S., Boertmann, D., Lange, R.,  
7 Nøjgaard, J.K., Harrison Roy, M., Simo, R., Skov, H., Massling, A. Regions of  
8 open water and melting sea ice drive new particle formation in North East  
9 Greenland. *Sci. Rep.* 8, 6109., 2018b  
10  
11 Dall'Osto, M., Beddows, D. C. S., Tunved, P., Harrison, R. M., Lupi, A., Vitale,  
12 V., Becagli, S., Traversi, R., Park, K.-T., Yoon, Y. J., Massling, A., Skov, H.,  
13 Lange, R., Strom, J., and Krejci, R.: Simultaneous measurements of aerosol  
14 size distributions at three sites in the European high Arctic, *Atmos. Chem.*  
15 *Phys.*, 19, 7377–7395, <https://doi.org/10.5194/acp-19-7377-2019>, 2019.  
16  
17 Davison, B., O'Dowd C., Hewitt Cc, Smith M, Harrison Roy M, Peel D., Wolf E.,  
18 Mulvaney R., Schwikowski M. and Baltensperger U., Dimethylsulfide and its  
19 oxidation products in the atmosphere of the Atlantic and southern oceans,  
20 *Atmos. Environ.*, 30, 1895-1906, 1996.  
21  
22 Doug McIlroy. Packaged for R by Ray Brownrigg, Thomas P Minka and  
23 transition to Plan 9 codebase by Roger Bivand. (2018). mapproj: Map  
24 Projections. R package version 1.2.6. [https://CRAN.R-](https://CRAN.R-project.org/package=mapproj)  
25 [project.org/package=mapproj](https://CRAN.R-project.org/package=mapproj)  
26  
27 Fiebig, M., Hirdman, D., Lunder, C. R., Ogren, J. A., Solberg, S., Stohl, A.,  
28 and Thompson, R. L.: Annual cycle of Antarctic baseline aerosol: controlled by  
29 photooxidation-limited aerosol formation, *Atmos. Chem. Phys.*, 14, 3083-3093,  
30 <https://doi.org/10.5194/acp-14-3083-2014>, 2014.  
31  
32 Frey, M. M., Norris, S. J., Brooks, I. M., Anderson, P. S., Nishimura, K., Yang,  
33 X., Jones, A. E., Nerentorp Mastromonaco, M. G., Jones, D. H., and Wolff, E.  
34 W.: First direct observation of sea salt aerosol production from blowing snow  
35 above sea ice, *Atmos. Chem. Phys. Discuss.*, [https://doi.org/10.5194/acp-](https://doi.org/10.5194/acp-2019-259)  
36 [2019-259](https://doi.org/10.5194/acp-2019-259), in review, 2019.  
37  
38 Fossum, K. N., Ovadnevaite, J., Ceburnis, D., Dall'Osto, M., Marullo, S.,  
39 Bellacicco, M., Simó, R., Liu, D., Flynn, M., Zuend, A., O'Dowd, C.:  
40 Summertime primary and secondary contributions to Southern Ocean cloud  
41 condensation nuclei, *Scientific Reports.*, 8, 13844, 2018.  
42  
43 Galí, M., Levasseur, M., Devred, E., Simó, R., and Babin, M.: Sea-surface  
44 dimethylsulfide (DMS) concentration from satellite data at global and regional  
45 scales, *Biogeosciences*, 15, 3497-3519, [https://doi.org/10.5194/bg-15-3497-](https://doi.org/10.5194/bg-15-3497-2018)  
46 [2018](https://doi.org/10.5194/bg-15-3497-2018), 2018.  
47  
48 Gantt, B. and Meskhidze, N.: The physical and chemical characteristics of  
49 marine primary organic aerosol: a review, *Atmos. Chem. Phys.*, 13, 3979–  
50 [3996](https://doi.org/10.5194/acp-13-3979-2013), doi:10.5194/acp-13-3979-2013, 2013.



- 1  
2 Giordano, M. R., Kalnajs, L. E., Avery, A., Goetz, J. D., Davis, S. M., and  
3 DeCarlo, P. F.: A missing source of aerosols in Antarctica – beyond long-  
4 range transport, phytoplankton, and photochemistry, *Atmos. Chem. Phys.*, 17,  
5 1–20, [https://doi.org/10.5194/acp-](https://doi.org/10.5194/acp-17-1-2017)  
6 [17-1-2017](https://doi.org/10.5194/acp-17-1-2017), 2017  
7  
8 Giordano, M. R., Kalnajs, L. E., Goetz, J. D., Avery, A. M., Katz, E., May, N.  
9 W., Leemon, A., Mattson, C., Pratt, K. A., and DeCarlo, P. F.: The importance  
10 of blowing snow to halogen-containing aerosol in coastal Antarctica: influence  
11 of source region versus wind speed, *Atmos. Chem. Phys.*, 18, 16689–16711,  
12 <https://doi.org/10.5194/acp-18-16689-2018>, 2018.  
13  
14 Gras, J. L. and Keywood, M.: Cloud condensation nuclei over the Southern  
15 Ocean: wind dependence and seasonal cycles, *Atmos. Chem. Phys.*, 17,  
16 4419–4432, <https://doi.org/10.5194/acp-17-4419-2017>, 2017.  
17  
18 Hamed, A., Korhonen, H., Sihto, S.-L., Joutsensaari, J., Jarvinen, H., Petaja,  
19 T., Arnold, F., Nieminen, T., Kulmala, M., Smith, J. N., Lehtinen, K. E. J., and  
20 Laaksonen, A.: The role of relative humidity in continental new particle  
21 formation, *J. Geophys. Res.*, 116, D03202, doi:10.1029/2010JD014186, 2011.  
22  
23 Hamilton, D. S., L. A. Lee, K. J. Pringle, C. L. Reddington, D. V. Spracklen,  
24 and K. S. Carslaw, Occurrence of pristine aerosol environments on a polluted  
25 planet, *P Natl Acad Sci USA*, 111, 18466–18471,  
26 doi:10.1073/pnas.1415440111, 2014  
27  
28 Hara K, Osada K, Nishita-Hara Cand Yamanouchi T 2011 Seasonal variations  
29 and vertical features of aerosol particles in the Antarctic troposphere *Atmos.*  
30 *Chem. Phys.* 11 5471–84  
31  
32 Herenz, P., Wex, H., Mangold, A., Laffineur, Q., Gorodetskaya, I. V., Fleming,  
33 Z. L., Panagi, M., and Stratmann, F.: CCN measurements at the Princess  
34 Elisabeth Antarctica research station during three austral summers, *Atmos.*  
35 *Chem. Phys.*, 19, 275–294, <https://doi.org/10.5194/acp-19-275-2019>, 2019.  
36  
37 Hodshire A L et al 2016 Multiple new-particle growth pathways observed at  
38 the USDOESouthern Great Plains field site *Atmos. Chem. Phys.* 16 9321–48  
39  
40 Hoppel, W.A., Frick, G.M., Fitzgerald, J.W., 1994. Marine boundary layer  
41 measurements of new-particle formation and the effects of non-precipitating  
42 clouds have on aerosol size distribution. *J. Geophys. Res.* 99, 14443–14459  
43  
44 Humphries, R. S., Schofield, R., Keywood, M. D., Ward, J., Pierce, J. R.,  
45 Gionfriddo, C. M., Tate, M. T., Krabbenhoft, D. P., Galbally, I. E., Molloy, S. B.,  
46 Klekociuk, A. R., Johnston, P. V., Kreher, K., Thomas, A. J., Robinson, A. D.,  
47 Harris, N. R. P., Johnson, R., and Wilson, S. R.: Boundary layer new particle  
48 formation over East Antarctic sea ice – possible Hg-driven nucleation?, *Atmos.*  
49 *Chem. Phys.*, 15, 13339–13364, <https://doi.org/10.5194/acp-15-13339-2015>,  
50 2015.



- 1  
2 Huang, J., Jaeglé, L., and Shah, V.: Using CALIOP to constrain blowing snow  
3 emissions of sea salt aerosols over Arctic and Antarctic sea ice, *Atmos. Chem.*  
4 *Phys.*, 18, 16253–16269, <https://doi.org/10.5194/acp-18-16253-2018>, 2018.  
5  
6  
7 Ito T 1993 Size distribution of Antarctic submicron aerosols *Tellus B*  
8 45 145–59  
9  
10 Jang, E., Park, K.-T., Yoon, Y. J., Kim, T.-W., Hong, S.-B., Becagli, S., raversi,  
11 R., Kim, J., and Gim, Y.: New particle formation events observed at the King  
12 Sejong Station, Antarctic Peninsula – Part 2: Link with the oceanic biological  
13 activities, *Atmos. Chem. Phys.*, 19, 7595–7608, [https://doi.org/10.5194/acp-](https://doi.org/10.5194/acp-19-7595-2019)  
14 [19-7595-2019](https://doi.org/10.5194/acp-19-7595-2019), 2019.  
15  
16 Järvinen, E., Virkkula, A., Nieminen, T., Aalto, P. P., Asmi, E., Lanconelli,  
17 C., Busetto, M., Lupi, A., Schioppo, R., Vitale, V., Mazzola, M., Petäjä, T.,  
18 Kerminen, V.-M., and Kulmala, M.: Seasonal cycle and modal structure of  
19 particle number size distribution at Dome C, Antarctica, *Atmos. Chem. Phys.*,  
20 13, 7473–7487, <https://doi.org/10.5194/acp-13-7473-2013>, 2013.  
21  
22 Jokinen, T., Sipilä, M., Kontkanen, J., Vakkari, V., Tisler, P., Duplissy, E.-M.,  
23 Junninen, H., Kangasluoma, J., Manninen, H. E., Petäjä, T., Kulmala,  
24 M., Worsnop, D. R., Kirkby, J., Virkkula, A., and Kerminen, V.-M.: Ion-induced  
25 sulfuric acid–ammonia nucleation drives particle formation in coastal  
26 Antarctica, *Sci. Adv.*, 4, eaat9744, <https://doi.org/10.1126/sciadv.aat9744>,  
27 2018.  
28  
29 Jung, J., Hong, S.-B., Chen, M., Hur, J., Jiao, L., Lee, Y., Park, K., Hahm, D.,  
30 Choi, J.-O., Yang, E. J., Park, J., Kim, T.-W., and Lee, S.: Characteristics of  
31 biogenically-derived aerosols over the Amundsen Sea, Antarctica, *Atmos.*  
32 *Chem. Phys. Discuss.*, <https://doi.org/10.5194/acp-2019-133>, in review, 2019.  
33  
34 Kalnay E., M. Kanamitsu, R. Kistler, W. Collins, D. Deaven, L. Gandin, M.  
35 Iredell, S. Saha, G. White, J. Woollen, Y. Zhu, M. Chelliah, W. Ebisuzaki, W.  
36 Higgins, J. Janowiak, K.C. Mo, C. Ropelewski, J. Wang, A. Leetmaa, R.  
37 Reynolds, R. Jenne, D. Joseph The NCEP/NCAR 40-year Reanalysis project  
38 *Bull. Am. Met. Soc.*, 77, pp. 437-471. [http://dx.doi.org/10.1175/1520-](http://dx.doi.org/10.1175/1520-0477(1996)077<0437:TNYRP>2.0.CO;2)  
39 [0477\(1996\)077<0437:TNYRP>2.0.CO;2](http://dx.doi.org/10.1175/1520-0477(1996)077<0437:TNYRP>2.0.CO;2), 1996  
40  
41 Kerminen, V.-M., Chen, X., Vakkari, V., Petäjä, T., Kulmala, M., and Bianchi,  
42 F.: Atmospheric new particle formation and growth: review of field observations,  
43 *Environ. Res. Lett.*, 13, 103003, <https://doi.org/10.1088/1748-9326/aadf3c>,  
44 2018.  
45  
46 Kim, J., Yoon, Y. J., Gim, Y., Kang, H. J., Choi, J. H., Park, K.-T., and Lee, B.  
47 Y.: Seasonal variations in physical characteristics of aerosol particles at the  
48 King Sejong Station, Antarctic Peninsula, *Atmos. Chem. Phys.*, 17, 12985–  
49 12999, <https://doi.org/10.5194/acp-17-12985-2017>, 2017.  
50



- 1  
2 Kim, J., Yoon, Y. J., Gim, Y., Choi, J. H., Kang, H. J., Park, K.-T., Park, J., and  
3 Lee, B. Y.: New particle formation events observed at King Sejong Station,  
4 Antarctic Peninsula – Part 1: Physical characteristics and contribution to cloud  
5 condensation nuclei, *Atmos. Chem. Phys.*, 19, 7583–7594,  
6 <https://doi.org/10.5194/acp-19-7583-2019>, 2019.  
7  
8 Koponen IK, Virkkula A, Hillamo R, Kerminen V-M andKulmalaM. Number  
9 size distributions of marine aerosols: observations during a cruise between  
10 the EnglishChannel and coast of Antarctica J. Geophys. Res. 107 4753, 2002  
11  
12 Koponen IK, Virkkula A, Hillamo R, Kerminen V-M andKulmalaM Number size  
13 distributions and concentrations of the continental summer aerosols in Queen  
14 Maud Land, Antarctica J. Geophys. Res. 108 4587, 2003  
15  
16 Korhonen, H., Carslaw, K. S., Spracklen, D. V., Mann, G., W.,and Woodhouse,  
17 M. T.: Influence of oceanic dimethyl sulfide emissions on cloud condensation  
18 nuclei concentrations and seasonality over the remote Southern Hemisphere  
19 oceans: A global model study, *J. Geophys. Res.-Atmos.*, 113, D15204,  
20 [doi:10.1029/2007JD009718](https://doi.org/10.1029/2007JD009718), 2008  
21  
22 Laaksonen, A., Kulmala, M., O'Dowd, C. D., Joutsensaari, J., Vaattovaara,P.,  
23 Mikkonen, S., Lehtinen, K. E. J., Sogacheva, L., DalMaso, M., Aalto, P.,  
24 Petäjä, T., Sogachev, A., Yoon, Y. J., Lihavainen,H., Nilsson, D., Facchini, M.  
25 C., Cavalli, F., Fuzzi, S.,Hoffmann, T., Arnold, F., Hanke, M., Sellegri, K.,  
26 Umann, B.,Junkermann, W., Coe, H., Allan, J. D., Alfarra, M. R., Worsnop,  
27 D. R., Riekkola, M. -L., Hyötyläinen, T., and Viisanen, Y.: Therole of VOC  
28 oxidation products in continental new particle formation, *Atmos. Chem. Phys.*,  
29 8, 2657–2665, [doi:10.5194/acp-8-2657-2008](https://doi.org/10.5194/acp-8-2657-2008), 2009  
30  
31 Liu, J., Dedrick, J., Russell, L. M., Senum, G. I., Uin, J., Kuang, C., Springston,  
32 S. R., Leaitch, W. R., Aiken, A. C., and Lubin, D.: High summertime aerosol  
33 organic functional group concentrations from marine and seabird sources at  
34 Ross Island, Antarctica, during AWARE, *Atmos. Chem. Phys.*, 18, 8571–8587,  
35 <https://doi.org/10.5194/acp-18-8571-2018>, 2018.  
36  
37 McCoy, D. T., Burrows, S. M., Wood, R., Grosvenor, D. P.,Elliott, S. M., Ma,  
38 P.-L., Rasch, P. J., and Hartmann, D.L.: Natural aerosols explain seasonal  
39 and spatial patterns of Southern Ocean cloud albedo, *Sci. Adv.*, 1, e1500157,  
40 <https://doi.org/10.1126/sciadv.1500157>, 2015  
41  
42 Murphy, D. M., Froyd, K. D., Bian, H., Brock, C. A., Dibb, J. E., DiGangi, J.  
43 P.,Diskin, G., Dollner, M., Kupc, A., Scheuer, E. M., Schill, G. P., Weinzierl, B.,  
44 illiamson, C. J., and Yu, P.: The distribution of sea-salt aerosol in the global  
45 troposphere, *Atmos. Chem. Phys.*, 19, 4093-4104,  
46 <https://doi.org/10.5194/acp-19-4093-2019>, 2019.  
47  
48 O'Dowd, C.D., Smith, M.H., Consterdine, I.E., Lowe, J.A., 1997a. Marine  
49 erosol, sea-salt, and the marinesulphur cycle—a short review. *Atmos. Environ.*  
50 31, 73–80, 1997a



- 1  
2 O'Dowd, CO, J. A. Lowe, M. H. Smith, B. Davison, C. N. Hewitt, R. M.  
3 Harrison, Biogenic sulphur emissions and inferred non-sea-salt-sulphate cloud  
4 condensation nuclei in and around Antarctica. *J. Geophys. Res. Atmos.* 102,  
5 12839–12854, 1997b  
6  
7 Quinn, P. K. and Bates, T. S.: The case against climate regulation via oceanic  
8 phytoplankton sulphur emissions, *Nature*,480(7375), 51–56,  
9 doi:10.1038/nature10580, 2011  
10  
11 Quinn, P. K., Collins, D. B., Grassian, V. H., Prather, K. A., and Bates, T. S.:  
12 Chemistry and Related Properties of Freshly Emitted Sea Spray Aerosol, *hem.*  
13 *Rev.*, 115, 4383–4399, doi:10.1021/cr500713g, 2015  
14  
15 Quinn, P. K., Coffman, D. J., Johnson, J. E., Upchurch, L. M., and Bates, T. S.:  
16 Small fraction of marine cloud condensation nuclei made up of sea spray  
17 aerosol, *Nat. Geosci.*, 10, 674–679, <https://doi.org/10.1038/ngeo3003>, 2017.  
18  
19 Rankin, A. M., and E. W. Wolff, A year-long record of size-segregated aerosol  
20 composition at Halley, Antarctica, *J. Geophys. Res.*, 108(D24), 4775,  
21 doi:10.1029/2003JD003993, 2003.  
22  
23 Reddington, C., Carslaw, K., Stier, P., Schutgens, N., Coe, H., Liu, D., Allan, J.,  
24 Pringle, K., Lee, L., and Yoshioka, M.: The Global Aerosol Synthesis and  
25 Science Project (GASSP): measurements and modelling to reduce uncertainty,  
26 *B. Am. Meteorol. Soc.*, 98.9, 1857–1877, 2017.  
27  
28 Richard A. Becker, Allan R. Wilks. R version by Ray Brownrigg.  
29 Enhancements by Thomas P Minka and Alex Deckmyn. (2018). maps: Draw  
30 Geographical Maps. R package version 3.3.0. [https://CRAN.R-](https://CRAN.R-project.org/package=maps)  
31 [project.org/package=maps](https://CRAN.R-project.org/package=maps)  
32  
33 Robert J. Hijmans (2019). raster: Geographic Data Analysis and Modeling. R  
34 package version 2.9-23. <https://CRAN.R-project.org/package=raster>  
35  
36 Roscoe, H. K., A. E. Jones, N. Brough, R. Weller, A. Saiz-Lopez, A. S.  
37 Mahajan, A. Schoenhardt, J. P. Burrows, and Z. L. Fleming (2015), Particles  
38 and iodine compounds in coastal Antarctica, *J. Geophys. Res. Atmos.*, 120,  
39 7144–7156, doi:10.1002/2015JD023301.  
40  
41 Saiz-Lopez, A., A. S. Mahajan, R. A. Salmon, S. J.-B. Bauguitte, A. E. Jones,  
42 H. K. Roscoe, and J. M. C. Plane (2007), Boundary layer halogens in coastal  
43 Antarctica, *Science*, 317, 348–351.  
44  
45 Sanchez, K. J., Chen, C.-L., Russell, L. M., Betha, R., Liu, J., Price, D. J.,  
46 Massoli, P., Ziemba, L. D., Crosbie, E. C., Moore, R. H., Müller, M., Schiller, S.  
47 A., Wisthaler, A., Lee, A. K. Y., Quinn, P. K., Bates, T. S., Porter, J., Bell, T.  
48 G., Saltzman, E. S., Vaillancourt, R. D., and Behrenfeld, M. J.: Substantial  
49 seasonal contribution of observed biogenic sulfate particles to cloud  
50 condensation nuclei, *Sci. Rep.*, 8, 3235, <https://doi.org/10.1038/s41598->



- 1 018-21590-9, 2018.  
2  
3 Schmale, J., Schneider, J., Nemitz, E., Tang, Y. S., Dragosits, U., Blackall, T.  
4 D., Trathan, P. N., Phillips, G. J., Sutton, M., and Braban, C. F.: Sub-Antarctic  
5 marine aerosol: dominant contributions from biogenic sources, *Atmos. Chem.  
6 Phys.*, 13, 8669–8694, <https://doi.org/10.5194/acp-13-8669-2013>, 2013.  
7  
8 Schönhardt, A., A. Richter, F. Wittrock, H. Kirk, H. Oetjen, H. K. Roscoe, and  
9 J. P. Burrows (2008), Observations of iodine monoxide (IO) columns from  
10 satellite, *Atmos. Chem. Phys.*, 8, 637–653 Shaw G.E. 1988 Antarctic  
11 aerosols: a review *Rev. Geophys.* 26 89–112  
12  
13 Sipilä, M., Sarnela, N., Jokinen, T., Henschel, H., Junninen, H., Kontkanen, J.,  
14 Ichners, S., Kangasluoma, J., Franchin, A., 5 Peräkylä, O., Rissanen, M.P., hn,  
15 M., Vehkamäki, H., Kurten, T., Berndt, T., Petäjä, T., Worsnop, D., Ceburnis, .,  
16 Kerminen, V.-M., Kulmala, M., O'Dowd, C., 2016. Molecular-scale evidence of  
17 aerosol particle formation via sequential addition of HIO<sub>3</sub>. *Nature* 537, 532–  
18 534. <https://doi.org/10.1038/nature19314>.  
19  
20 Shaw, G. E.: Considerations on the Origin and Properties of the Antarctic  
21 Aerosol, *Rev. Geophys.*, 17, 1983–1998, 1988.  
22  
23 Teinilä, K., Frey, A., Hillamo, R., Tülp, H. C., and Weller, R.: A study of the  
24 sea-salt chemistry using size-segregated aerosol measurements at coastal  
25 Antarctic station Neumayer, *Atmos. Environ.*, 96, 11–19, 2014.  
26  
27 Udisti, R., Dayan, U., Becagli, S., Busetto, M., Frosini, D., Legrand, M.,  
28 Lucarelli, F., Preunkert, S., Severi, M., Traversi, R., and Vitale, V.: Sea spray  
29 aerosol in central Antarctica. Present atmospheric behaviour and implications  
30 for paleoclimatic reconstructions, *Atmos. Environ.*, 52, 109–  
31 120, <https://doi.org/10.1016/j.atmosenv.2011.10.018>, 2012.  
32  
33 Vallina, S. M. and Simó, R.: Re-visiting the CLAW hypothesis, *Environ. Chem.*,  
34 4, 384–387, <https://doi.org/10.1071/EN07055>, 2007.  
35  
36 Virkkula, A., Teinilä, K., Hillamo, R., Kerminen, V.-M., Saarikoski, S., Aurela,  
37 M., Viidanoja, J., Paatero, J., Koponen, I. K., Kulmala, M.: Chemical  
38 composition of boundary layer aerosol over the Atlantic Ocean and at an  
39 Antarctic site, *Atmos. Chem. Phys.*, 6, 3407–3421, 2006.  
40  
41 Yang, X., Frey, M. M., Rhodes, R. H., Norris, S. J., Brooks, I. M., Anderson, P.  
42 S., Nishimura, K., Jones, A. E., and Wolff, E. W.: Sea salt aerosol production  
43 via sublimating wind-blown saline snow particles over sea ice:  
44 parameterizations and relevant microphysical mechanisms, *Atmos. Chem.  
45 Phys.*, 19, 8407–8424, <https://doi.org/10.5194/acp-19-8407-2019>, 2019.  
46  
47 Weller, R., Minikin, A., Wagenbach, D., and Dreiling, V.: Characterization of  
48 the inter-annual, seasonal, and diurnal variations of condensation particle  
49 concentrations at Neumayer, Antarctica, *Atmos. Chem. Phys.*, 11, 13243–  
50 13257, <https://doi.org/10.5194/acp-11-13243-2011>, 2011.



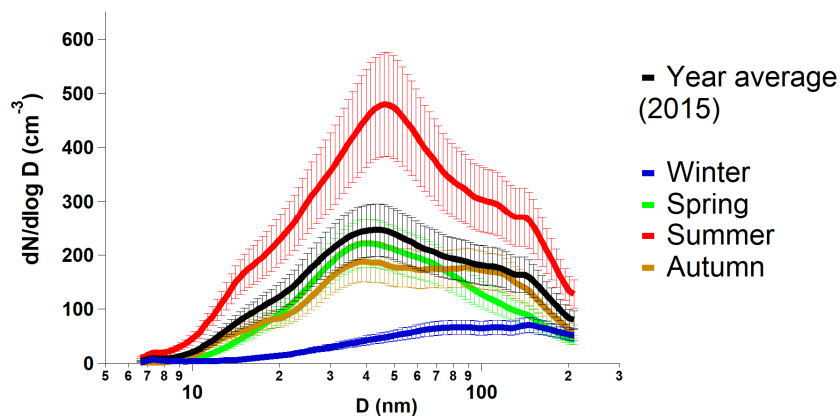
1  
2 Weller, R., Schmidt, K., Teinilä, K., and Hillamo, R.: Natural new particle  
3 formation at the coastal Antarctic site Neumayer, *Atmos. Chem. Phys.*, 15,  
4 11399–11410, <https://doi.org/10.5194/acp-15-11399-2015>, 2015.  
5  
6 Weller, R., Legrand, M., and Preunkert, S.: Size distribution and ionic  
7 composition of marine summer aerosol at the continental Antarctic site  
8 Kohnen, *Atmos. Chem. Phys.*, 18, 2413–2430, <https://doi.org/10.5194/acp-18-2413-2018>, 2018.  
9  
10  
11 Xu, G. J., Gao, Y., Lin, Q., Li, W., and Chen, L. Q.: Characteristics of water-  
12 soluble inorganic and organic ions in aerosols over the Southern Ocean and  
13 coastal East Antarctica during austral summer, *J. Geophys. Res.-Atmos.*, 118,  
14 13303–13318, <https://doi.org/10.1002/2013jd019496>, 2013.  
15  
16 Zorn, S. R., Drewnick, F., Schott, M., Hoffmann, T., and Borrmann, S.:  
17 characterization of the South Atlantic marine boundary layer aerosol using an  
18 aerodyne aerosol mass spectrometer, *Atmos. Chem. Phys.*, 8, 4711–4728,  
19 <https://doi.org/10.5194/acp-8-4711-2008>, 2008.  
20  
21  
22  
23  
24  
25  
26  
27  
28  
29  
30  
31  
32  
33  
34  
35  
36  
37  
38  
39  
40





1  
2  
3  
4  
5  
6  
7  
8

## LIST OF FIGURES



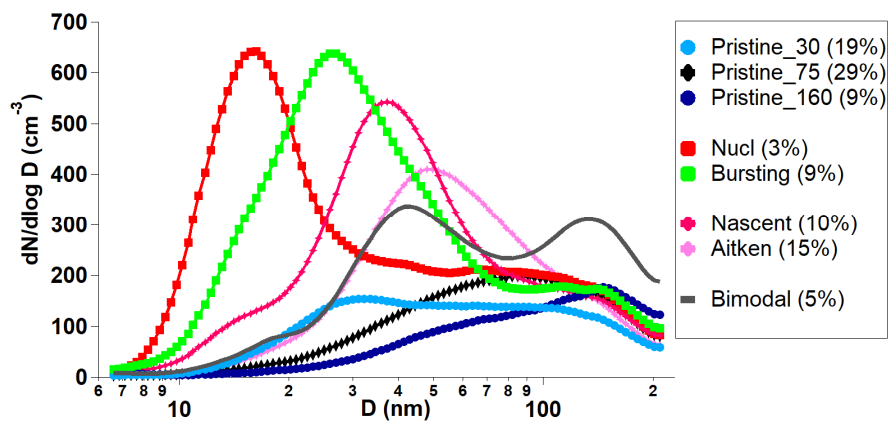
9  
10  
11  
12  
13  
14  
15  
16  
17  
18  
19  
20  
21  
22  
23  
24

**Figure 1** Seasonal mean aerosol size distribution measured by the SMPS at Halley VI research station over the year 2015. The error bars represent the standard deviation of the measurements from the mean value.



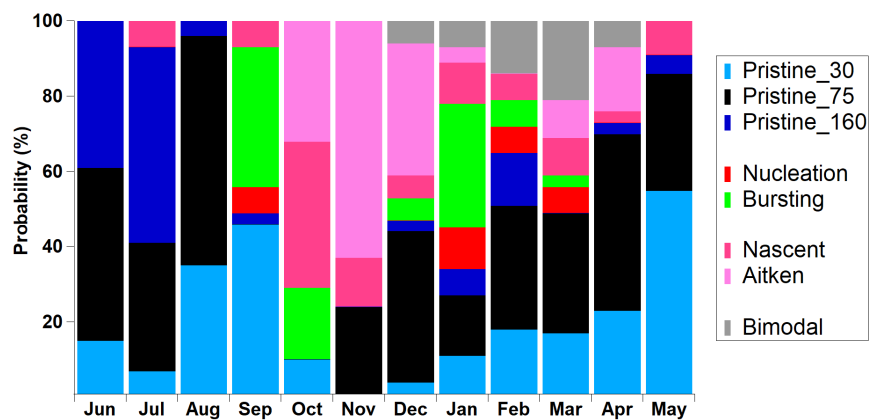


1  
2



3  
4  
5  
6

(a)



7  
8  
9

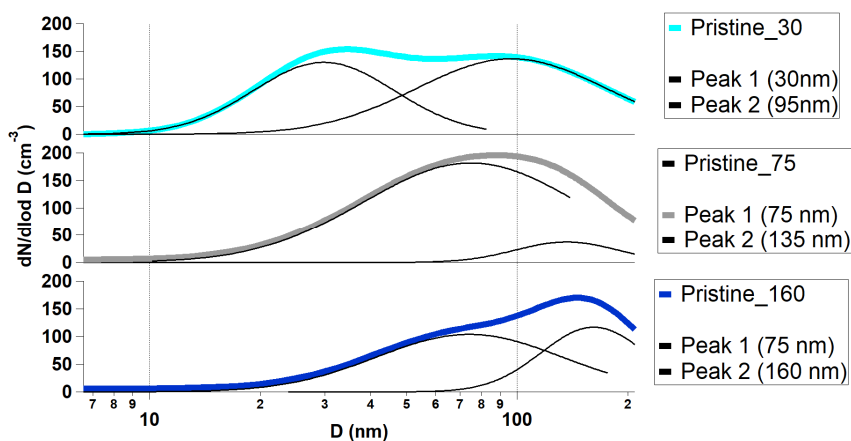
(b)

10 **Figure 2** (a) Size distributions of the 8 k-means clusters and (b) annual  
11 frequency distributions of the six aerosol categories

12  
13  
14  
15



1  
2  
3  
4  
5  
6  
7  
8

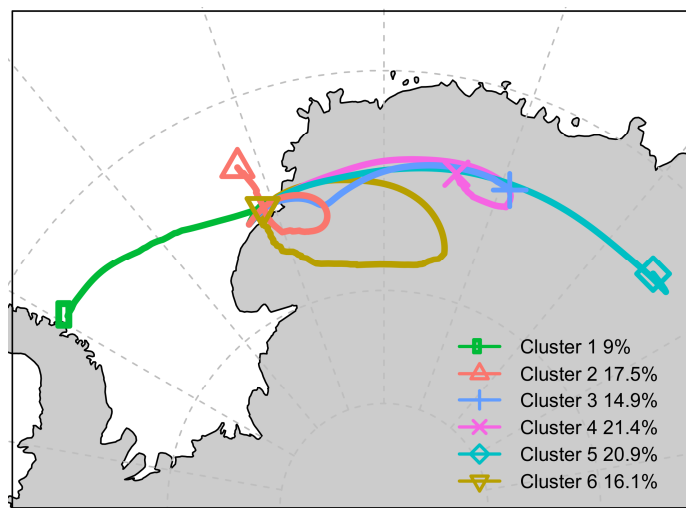


9  
10  
11  
12  
13  
14  
15  
16  
17  
18  
19  
20  
21  
22  
23  
24

**Figure 3** Peak fitting of the 3 pristine K-means aerosol categories.

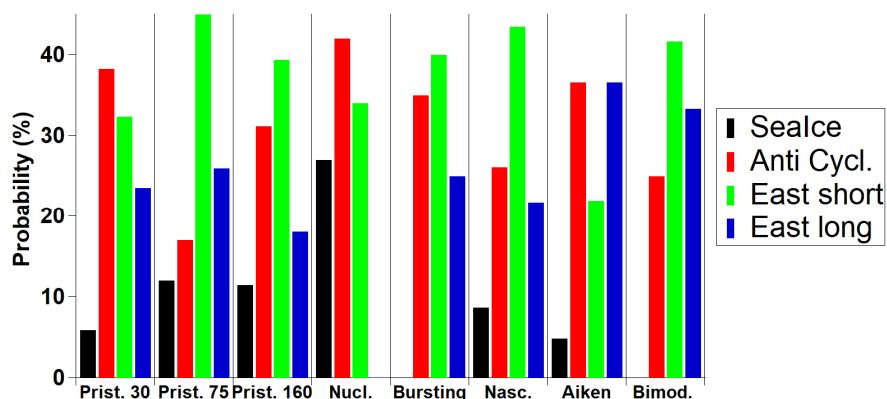


1  
 2  
 3



4  
 5

(a)

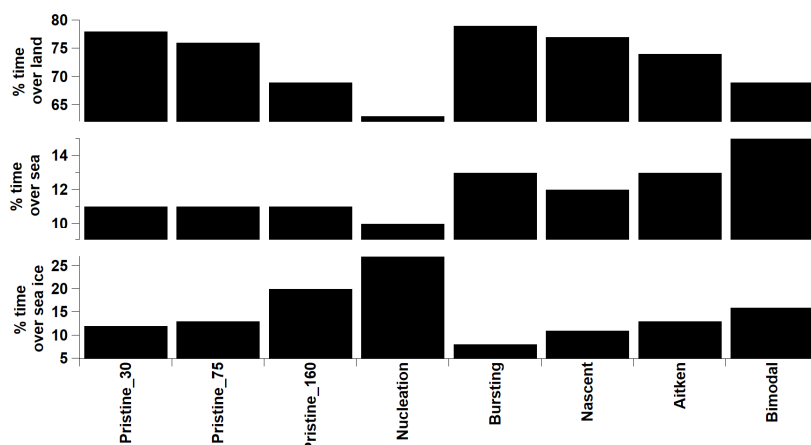


6  
 7

(b)

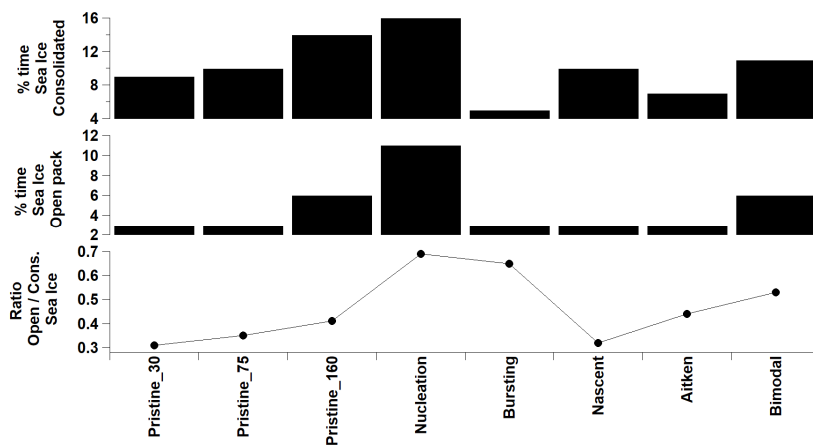
8 **Figure 4 (a)** Air mass analysis of air mass back trajectories arriving at Halley  
 9 during the year 365 (hourly resolution) and **(b)** relative contribution for each  
 10 aerosol category. Groups in (b) are : Sea Ice (1), Anti Cycl (2,6), East short  
 11 (3,4) and east long (5),

12  
 13  
 14



1  
 2  
 3  
 4  
 5

(a)



6  
 7  
 8  
 9

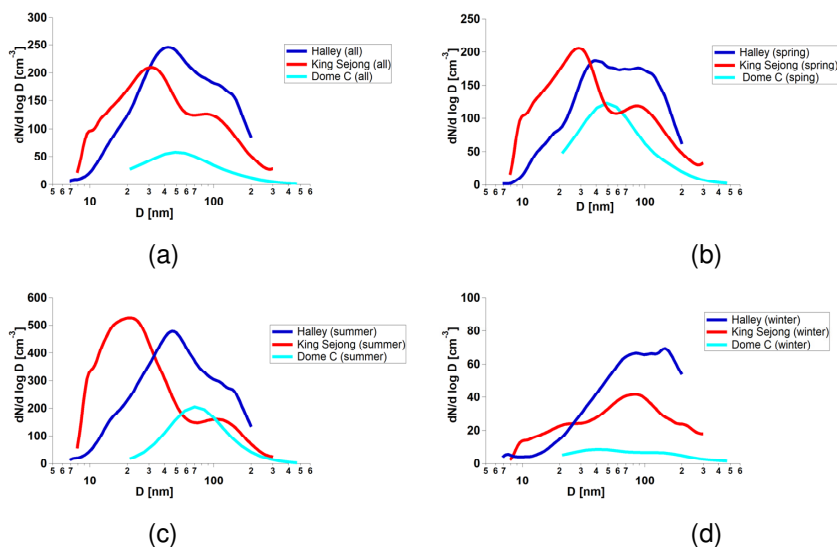
(b)

10 **Figure 5** (a) Percentages of air masses over land, sea, and sea ice for the 8  
 11 K-means aerosol categories and (b) percentages of consolidated and open  
 12 pack sea ice, and open pack / consolidated ratio.

13  
 14  
 15



1  
2  
3



4

5

6

7

8

9 **Figure 6.** Average size-resolved particle size distributions simultaneously  
10 measured during the year 2015 at Halley, Dome C and King Sejong stations  
11 for (a) May-December (8 months), (b) spring (Sep., Oct., Nov., 3 months), (c)  
12 summer (December, 1 month) and (d) winter (Jun., Jul., Aug., 3 months).

13

14

15

16

17

18

19

20

21

22

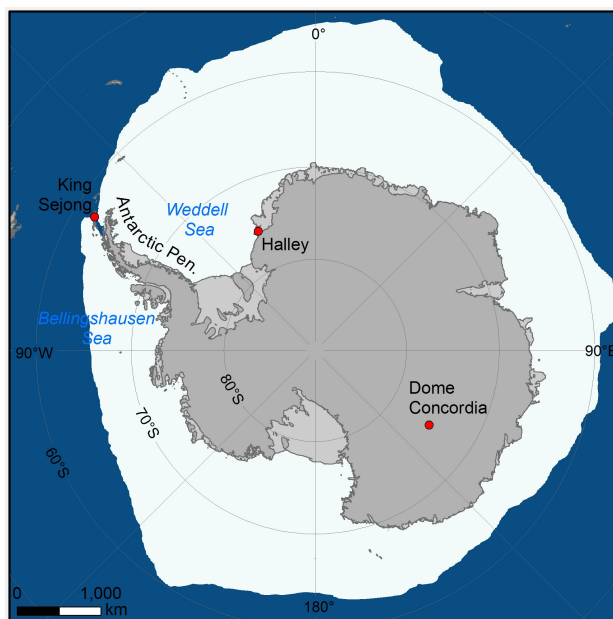
23

24

25



1  
2

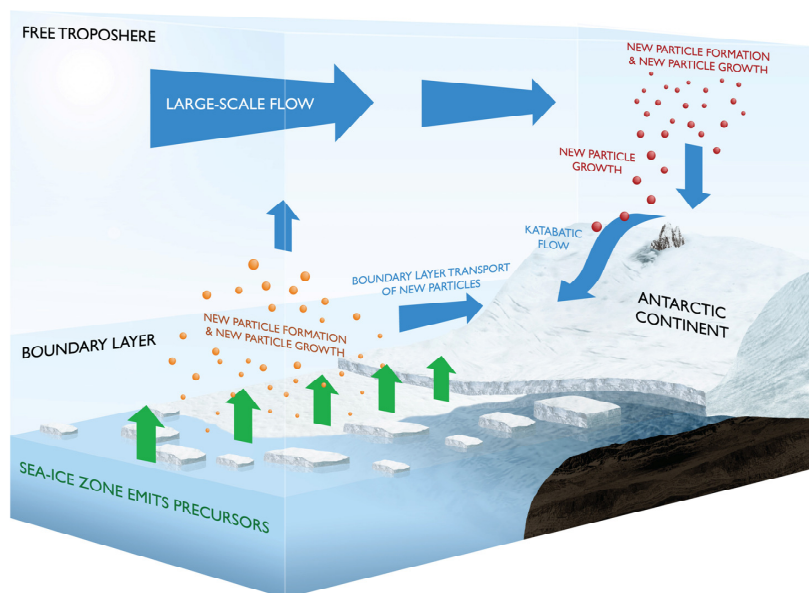


3  
4  
5  
6  
7  
8  
9  
10  
11  
12  
13  
14  
15  
16  
17  
18  
19  
20

**Figure 7.** Map with locations of Antarctic monitoring stations considered in Figure 6. Please note that the sea ice extent is the median September extent from 1981-2010 (data are from NSIDC - <https://nsidc.org/data/g02135>).



1



2

3

4 **Figure 8** Schematic illustrations of the ultrafine New Particle Formation (NPF)  
5 and New Particle Growth (NPG) aerosols in Antarctica.

6

7

8

9

10

11

12

13

14

15

16

17

18